QT# 47438 QA:NA

Impact of Quaternary Climate on Seepage at Yucca Mountain, Nevada

Joseph F. Whelan
U.S. Geological Survey
PO Box 25046, MS 963
Denver, CO 80225
jfwhelan@usgs.gov

James B. Paces
U.S. Geological Survey
PO Box 25046, MS 963
Denver, CO 80225
jbpaces@usgs.gov

Leonid A. Neymark
U.S. Geological Survey
PO Box 25046, MS 963
Denver, CO 80225
lneymark@usgs.gov

Axel K. Schmitt
Dept. Earth and Space Sciences
595 Charles Young Dr. East, Box 951567
Univ. California, Los Angeles
Los Angeles, CA 90095
axel@argon.ess.ucla.edu

Marty Grove
Dept. Earth and Space Sciences
595 Charles Young Dr. East, Box 951567
Univ. California, Los Angeles
Los Angeles, CA 90095
marty@argon.ess.ucla.edu

Abstract – Uranium-series ages, oxygen-isotopic compositions, and uranium contents were determined in outer growth layers of opal and calcite from 0.5- to 3-centimeter-thick mineral coatings hosted by lithophysal cavities in the unsaturated zone at Yucca Mountain, Nevada, the proposed site of a permanent repository for high-level radioactive waste. Micrometer-scale growth layering in the minerals was imaged using a cathodoluminescence detector on a scanning electron microscope. Determinations of the chemistry, ages, and delta oxygen-18 values of the growth layers were conducted by electron microprobe analysis and secondary ion mass spectrometry techniques at spatial resolutions of 1 to about 20 micrometers (μm) and 25 to 40 micrometers, respectively. Growth rates for the last 300 thousand years (k.y.) calculated from about 300 new high-resolution uranium-series ages range from approximately 0.5 to 1.5 μm/k.y. for 1- to 3-centimeter-thick coatings, whereas coatings less than about 1-centimeter-thick have growth rates less than 0.5 μm/k.y. At the depth of the proposed repository, correlations of uranium concentration and delta oxygen-18 values with regional climate records indicate that unsaturated zone percolation and seepage water chemistries have responded to changes in climate during the last several hundred thousand years.

I. INTRODUCTION

Seepage of water into emplacement drifts of the proposed high-level radioactive waste repository at Yucca Mountain, Nevada (Fig. 1), could cause corrosion of waste canisters and transport of radioactive contaminants. During the past million years (m.y.), mean annual temperature and precipitation have fluctuated between warmer, drier interglacial climates and colder, wetter glacial climates [2-5], with past climates producing infiltration fluxes from 5 to 10 times greater than present day values, as estimated from relations between net infiltration (Fig. 4-6 [6]) and mean annual precipitation up to 500 millimeters/year for full glacial climates (Table 6-3) [6]. Understanding how percolation and seepage fluxes deeper in the unsaturated zone (UZ), at the level of the proposed repository, responded to these climate changes will help to reduce uncertainties in predictions of repository performance.

Meteoric water percolating downward through the 12.7- to 12.8-million-year-old [7] welded Tiva Canyon and Topopah Spring Tuffs has deposited secondary minerals (dominantly opal and calcite) in fractures and cavities [8-10]. Because less than 10 percent of open fractures and cavities contain secondary minerals, the deposits are attributed to seepage water moving down fracture flow paths rather than to matrix percolation [9, 10]. Although secondary minerals formed over the past 10 m.y. or more [9, 11], late-stage opal and calcite deposited in the last 2 to 4 m.y. [12] are most relevant to understanding the probable range of UZ hydrologic conditions during the next million years. Due to the slow growth rates of the secondary mineral deposits (less than 5 micrometers [μm] per thousand years [k.y.]), high spatial-resolution analytical techniques, such as secondary ion mass spectrometry (SIMS) and electron microprobe analysis (EMPA), are required to determine the timing and geochemical variability of mineral deposition [9, 13-15]. This paper discusses new uranium (U)-series ages, determined by SIMS, that better characterize the late-stage growth histories of lithophysal-cavity-hosted secondary minerals (lithophysal cavities are gas-exsolution cavities formed during the initial cooling of the tuffs [10]). Opal and calcite $\delta^{18}O$ values and U concentrations determined by SIMS, and magnesium (Mg) concentrations determined by EMPA, were used to evaluate the relations between past climate variations and UZ seepage at the level of the proposed repository.

II. METHODS

Cathodoluminescence (CL) and EMPA were used to investigate micrometer-scale growth layering of the late-stage opal and calcite. High-spatial resolution U-series (^{230}Th/U and ^{234}U/^{238}U) ages of Quaternary opal were determined using SIMS with 25- to 30-μm-diameter spot analyses at the Stanford/USGS SIMS facility at Stanford University in Palo Alto, or by sequential microdigestion of opal surfaces with hydrofluoric acid, followed by analysis of the solute by thermal ionization mass spectrometry. The details of these analytical procedures are described in Paces and others [13]. Microstratigraphic depths of dated layers were measured perpendicular to growth layering imaged by CL and combined with U-series dates to calculate rates of opal growth.

The δ^{18}O values of calcite growth layers coincident with dated opal layers, and of opal growth layers directly, were determined by SIMS at the National Ion Microprobe Facility at the University of California, Los Angeles. The analysis spots had approximately 40 μm-diameters and data collection and reduction followed procedures described by Treble and others [16]. Oxygen isotope compositions are reported in δ-notation as the permil (‰) deviations from the international standard VSMOW; the accepted $\delta^{18}O_{VSMOW}$ value for NBS-19 is 28.65‰ [17]. The average corrected δ^{18}O of NBS-19 during the course of the data collection was 28.63 ± 0.30‰ (2 sigma [σ]).

II. RESULTS

II.A. Compositional Growth Layering

Micrometer-scale growth layering of late-stage opal and calcite can be detected by various methods [8, 10]. Wilson and others [18] showed that Mg concentrations in late-stage calcite range from less than 0.05 to 1 weight percent and define complex growth layering. EMPA mapping of Mg, manganese (Mn), strontium (Sr), and iron (Fe) concentrations confirmed the oscillatory variation of Mg concentration in calcite. However, the other elements were commonly below EMPA detection limits and corresponding variations, if present, could not be resolved. Oscillations of CL intensity, observed in scanning electron microscope (SEM) images of late-stage opal and calcite (Figs. 2 and 3), also define growth layering. Opal CL intensities in these samples strongly correlate with U concentrations, which range from approximately 4 to 450 micrograms per gram (μg/g) [19], whereas growth layering in calcite is caused by variations in trace element concentrations that act as CL activators (Mn^{2+}) or quenchers (Fe^{2+}) [20]. EMPA mapping also revealed growth-correlated fluctuations of Mg concentration in opal at about the same scale as the CL banding. Preliminary interpretation of these maps indicates that Mg and U concentrations in opal are inversely correlated. Similarly oriented growth layering in both opal and calcite, together with stepped or intercuspate contact relations in many samples, indicate more-or-less concurrent growth of the two phases (Figs. 2 and 3).

II.B. U-series Ages and Growth Rates

Approximately 300 new SIMS U-series ages have been determined on profiles across late-stage opal from eight lithophysal-cavity-hosted secondary mineral deposits within the proposed repository horizon. The ages range from about 20 to 1,500 thousand years ago (ka) and increase with microstratigraphic depth. For 1- to 3-centimeter (cm)-thick coatings, growth rates calculated for the last 300 k.y. range from approximately 0.5 to 1.5 μm/k.y., whereas coatings less than about 1-cm-thick have growth rates less than 0.5 μm/k.y. Opal growth rates determined from the best-constrained age-depth profiles are remarkably constant, varying by only 20 to 30 percent during the last 300 k.y., despite the presumably large differences in infiltration between glacial and interglacial climates. Growth rates for mineral coatings dominated by calcite with only minor intercalated opal are similar to rates for thick opal accumulations. The 30-μm spatial resolution of SIMS analyses cannot resolve short term (less than 10 k.y.) changes of growth rate. Nonetheless, preliminary numerical simulations of growth rate profiles determined using overlapping 25-μm-diameter analysis spots, resulting in an interpolated spatial resolution of 12.5 μm, indicate that depositional hiatuses greater than about 10 k.y. should be detectable.

Microdigestion ^{230}Th/U ages from 2- to 4-μm-thick opal layers produced progressively older ages from 7.3±0.7 to 37.1±2.3 ka from the outer surface of an opal coating to a depth of about 22 μm. Age-depth relations at this scale of resolution may indicate faster opal growth rates (1.2±0.4 μm/k.y.) during the last full glacial period and slower rates (0.35±0.19 μm/k.y.) during the more recent glacial-interglacial transition. Both Holocene ages for outermost microdigestions and non-zero intercepts for age relative to microstratigraphic depth regressions indicate that mineral growth ceased during the most recent dry-climate period [13].

II.C. Oxygen Isotopes in Late-Stage Calcite

Cathodoluminescence images showing late-stage growth layering were used to correlate contemporaneous opal and calcite layers and to locate analysis spots in calcite for SIMS determinations of calcite $\delta^{18}O$ values. Late-stage calcite $\delta^{18}O$ values in samples of deposits from the Topopah Spring Tuff range from 15.4 to 18.2‰ (±0.3‰, 2σ). The feasibility of using SIMS to measure $\delta^{18}O$ values in opal also was tested. In opal (hydrated silicon dioxide [$SiO_2 \cdot nH_2O$]), oxygen can reside in silicate tetrahedral sites or as structural hydroxide (OH^-) or water (H_2O), all having different oxygen bonding energies and different isotopic compositions [21]. In spite of these complications, the $\delta^{18}O$ values of opal layers had within-run precision that was similar to calcite $\delta^{18}O$ determinations, excellent reproducibility (±0.20‰, 2σ) for paired analyses of individual opal layers (Table I), and a positive correlation ($r^2 = 0.77$) between the $\delta^{18}O$ values of 7 pairs of corresponding opal and calcite growth layers (Figs. 3 and 4). These promising results suggest that $\delta^{18}O$ value and U-series ages can be determined from individual opal layers at 30 μm spatial resolution. The direct relation between age and $\delta^{18}O$ value determined within discrete grains and a single mineral would eliminate the uncertainty associated with attempting to correlate opal and calcite growth-layer microstratigraphies across grain boundaries (see Fig. 3).

III. DISCUSSION AND CONCLUSIONS

Profiles of relative U concentration (approximated by CL intensity) versus microstratigraphic depth in opal samples were normalized for different growth rates using SIMS U-series ages; one of these is shown in figure 4. Well-dated profiles from five separate deposits in different parts of the proposed repository horizon show similar temporal variations. High-U opal formed during three separate periods over the last 300 k.y., all of which correspond to relatively warm interglacial climate states, based on $\delta^{18}O$ variations observed in the regional climate record at Devils Hole [22, 23] (Fig. 4). Age-normalized $\delta^{18}O$ variations in late-stage opal and calcite in the UZ also are consistent with the calcite $\delta^{18}O$ record at Devils Hole (Fig. 4). These correlations of U concentration and $\delta^{18}O$ values with regional climate records indicate that UZ percolation and seepage water chemistries have responded to changes in climate during the last several hundred thousand years.

The deposition of free-standing secondary opal and calcite in UZ lithophysal cavities indicates seepage into those lihtophysae, probably from fracture-hosted flow paths. Most samples of surface runoff and UZ flow (pore water from non-zeolitized units, seepage, and perched water) are near saturation with respect to both opal and calcite [9, 24-27]. Deposition of opal and calcite, therefore, requires only evaporation or carbon dioxide (CO_2) degassing of seepage water [8–10]. This mechanism is consistent with the concurrent deposition and similar growth rates of opal and calcite. Free movement of gases through the welded tuff fracture network is likely – down-hole pneumatic testing shows that changes in atmospheric pressure are transmitted to the repository horizon with little attenuation or phase lagging [28]. Therefore, water vapor and CO_2 evolved during opal and calcite deposition should readily escape from lithophysal cavities; if they could not escape, $H_2O_{(v)}$ and CO_2 saturation of the cavity atmosphere would inhibit mineral growth. Consequently, the absence of secondary minerals in 90 percent or more of the fracture or lithophysal cavity openings in the UZ must reflect a lack of seepage into those openings rather than differences in gas permeability.

Marshall and others [26] presented an equilibrium geochemical model of mineral deposition at Yucca Mountain that assumed seepage flux was an important control on mineral growth rates. Evidence used to support this model came from other studies of UZ environments where both water fluxes and mineral growth rates were measured [29, 30]. The much slower growth rates measured for Yucca Mountain UZ minerals indicate less seepage than other depositional environments. The 0.5 to 1.5 μm/k.y. growth rates determined for material deposited in the last 300 k.y. are similar to the rates of 0.3 to 1.8 μm/k.y. calculated using the 0.3 cm (median) and 1.8 cm (95^{th} percentile) coating thicknesses reported by Marshall and others [26] and an assumed 10 m.y. depositional history. The consistency between measured Quaternary growth rates and long-term growth rates [26] is interpreted as evidence for the long-term hydrologic stability of the deep UZ environment. Long-term average Miocene growth rates (1 to 5 μm/k.y.) of opal and calcite in older portions of the same samples [11] are slightly faster than the Quaternary growth rates (0.5 to 1.5 μm/k.y.) in the late-stage. This difference may reflect an overall decrease in seepage flux as climate shifted from wetter conditions in the Miocene to more arid conditions in the Quaternary [13]. A direct relation between seepage flux and mineral growth rate also is supported by sequential opal microdigestions of a single opal grain that indicated higher growth rates during the last full glacial climate (dates between 37 and 25 ka), lower growth rates during the last glacial transition period (dates between 25 and 7 ka), and a cessation of growth during the present interglacial climate stage [13]. Furthermore, thinner coatings have lower growth rates, which may indicate that percolation fluxes at these sites only infrequently exceeded thresholds allowing seepage of fracture flow or, alternatively, that there was less evaporation/CO_2 degassing at these sites. The ages reported here indicate that seepage fluxes and secondary mineral growth rates are proportional within a given lithophysal cavity; i.e., relative differences in growth rate during the last two to three climate cycles (300 k.y.) reflect relative differences in seepage flux. Changes in opal and calcite U and Mg contents and $\delta^{18}O$ compositions during the last 300 k.y. record shifts in seepage chemistry that correlate with variations in late Quaternary climate conditions. However, at current levels of analytical resolution mineral growth rates in the Topopah Spring Tuff lithophysal cavities have remained relatively constant. These results indicate that changes in mean annual precipitation and temperature between wetter and drier climate states during the past 300 k.y., which should have produced large variations in near-surface infiltration, did not produce similarly large variations in seepage flux at the proposed repository horizon.

ACKNOWLEDGMENTS

This study was done by the U.S. Geological Survey in cooperation with the U.S. Department of Energy under Interagency Agreement DE-AI28-02RW12167. Heather Lowers and Isabelle Brownfield of the USGS-Denver Microbeam Laboratory provided expert assistance for CL imaging and EMPA mapping.

REFERENCES

1. W.C. DAY, C.J. POTTER, D.S. SWEETKIND, R.P. DICKERSON, and C.A. SAN JUAN "Bedrock geologic map of the central block area, Yucca Mountain, Nye County, Nevada" : *U.S. Geological Survey Geologic Investigations Series* **I-2601**, 15 p., 2 map sheets + 1 pamphlet, 15 p. (1998).
2. W.G. SPAULDING, "Vegetation and Climates of the Last 45,000 Years in the Vicinity of the Nevada Test Site, South-Central Nevada," *U.S. Geological Survey Professional Paper* **1329**, 83 p. (1985).
3. R.M. FORESTER, J.P. BRADBURY, C. CARTER, A. ELVIDGE, M. HEMPHILL, S.C. LUNDSTROM, S.A. MAHAN, B.D. MARSHALL, L.A. NEYMARK, J.B. PACES, S. SHARPE, J.F. WHELAN, and P. WIGAND, "The Climatic and Hydrologic History of Southern Nevada During the Late Quaternary," *U.S. Geological Survey Open-File Report* **98-635**, 63 p. (1999).
4. R.S. THOMPSON, K.H. ANDERSON, and P.J. BARTLEIN, "Quantitative Paleoclimatic Reconstructions from Late Pleistocene Plant Macrofossils of the Yucca Mountain Region," *U.S. Geological Survey Open-File Report* **99-338**, 38 p. (1999).
5. S. SHARPE, "Future Climate Analysis—10,000 Years to 1,000,000 Years After Present," MOD-01-001, REV 1, ACC: MOL.20030407.0055, 80 p., Desert Research Institute, Reno, Nevada (2003). Accessed March 1, 2006 at http://www.lsnnet.gov (LSN# DEN001232582)
6. BECHTEL SAIC COMPANY, LLC, "Technical Basis Document No. 1: Climate and Infiltration," REV 1, ACC: MOL.20040804.0292, 206 p., Bechtel SAIC Company, LLC, Las Vegas, Nevada (2004). http://www.ocrwm.doe.gov/documents/43225_tbd/index.htm
7. D.A. SAWYER, R.J. FLECK, M.A. LANPHERE, R.G. WARREN, D.E. BROXTON, and M.R. HUDSON, "Episodic Caldera Volcanism in the Miocene Southwestern Nevada Volcanic Field—Revised Stratigraphic Framework, $^{40}Ar/^{39}Ar$ Geochronology, and Implications for Magmatism and Extension," *Geological Society of America Bulletin* **106**, 1304 (1994).

8. J.F. WHELAN, D.T. VANIMAN, J.S. STUCKLESS, and R.J. MOSCATI, *Paleoclimatic and Paleohydrologic Records from Secondary Calcite—Yucca Mountain, Nevada, Proc. Fifth Int'l High-Level Radioactive Waste Management Conference, Las Vegas, Nevada, May 22-26, 1994*, p. 2738, American Nuclear Society, La Grange Park, Illinois (1994).

9. J.B. PACES, L.A. NEYMARK, B.D. MARSHALL, J.F. WHELAN, and Z.E. PETERMAN, "Ages and Origins of Calcite and Opal in the Exploratory Studies Facility Tunnel, Yucca Mountain, Nevada," *U.S. Geological Survey Water-Resources Investigation Report* **01-4049**, 95 p. (2001).

10. J.F. WHELAN, J.B. PACES, and Z.E. PETERMAN, "Physical and Stable-Isotope Evidence for Formation of Secondary Calcite and Silica in the Unsaturated Zone, Yucca Mountain, Nevada," *Applied Geochem.* **17**, 735 (2002).

11. L.A. NEYMARK, Y. V. AMELIN, J.B. PACES, and Z.E. PETERMAN, "U-Pb Ages of Secondary Silica at Yucca Mountain, Nevada: Implications for the Paleohydrology of the Unsaturated Zone," *Applied Geochem.* **17**, 709 (2002).

12. J.F. WHELAN and R.J. MOSCATI, *9 m.y. Record of Southern Nevada Climate from Yucca Mountain Secondary Minerals, Proc. Eighth Int'l High-Level Radioactive Waste Management Conference, Las Vegas, Nevada, May 11-14, 1998*, p. 12, American Nuclear Society, La Grange Park, Illinois (1998).

13. J.B. PACES, L.A. NEYMARK, J.L. WOODEN, and H.M. PERSING, "Improved Spatial Resolution for U-Series Dating of Opal at Yucca Mountain, Nevada, USA, Using Ion-Microprobe and Microdigestion Methods," *Geochim. Cosmochim. Acta* **68**, 1591 (2004).

14. L.A. NEYMARK, Y. V. AMELIN, and J.B. PACES, "^{206}Pb-^{230}Th-^{234}U-^{238}U and ^{207}Pb-^{235}U Geochronology of Quaternary Opal, Yucca Mountain, Nevada," *Geochim. Cosmochim. Acta* **64**, 2913 (2000).

15. L.A. NEYMARK, and J.B. PACES, "Consequences of Slow Growth for ^{230}Th/U Dating of Quaternary Opals, Yucca Mountain, NV, USA," *Chemical Geology* **164**, 143 (2000).

16. P.C. TREBLE, J.C. CHAPPELL, M.K. GAGAN, T.M. HARRISON, and K.D. MCKEEGAN. "In Situ Measurement of Seasonal ^{18}O Variations and Analysis of Isotopic Trends in a Precisely Dated Modern Speleothem from Southwest Australia," *Earth Planet. Sci. Lett.* **233**, 17 (2005).

17. T.B. COPLEN. "New guidelines for reporting stable hydrogen, carbon, and oxygen isotope-ratio data," *Geochim. Cosmochim. Acta,* **60**, 3359 (1996).

18. N.S.F. WILSON, J.S. CLINE, and Y.V. AMELIN, "Origin, Timing, and Temperature of Secondary Calcite-Silica Mineral Formation at Yucca Mountain, Nevada," *Geochim. Cosmochim. Acta* **67**, 1145 (2003).

19. J.B. PACES, L.A. NEYMARK, and J.L. WOODEN, "Variations in Pleistocene Fracture Flow at Yucca Mountain, Nevada, Investigated by Ion Microprobe U-series Dating and Cathodoluminescence of Unsaturated-Zone Opal," *Geol. Soc. Amer. Abst. with Prog.* **36**, 108 (2004).

20. D.J. MARSHALL, *Cathodoluminescence of Geological Materials*, Unwin Hyman, Boston, MA, 146 p. (1988).

21. M. HAIMSON and L.P. KNAUTH, "Stepwise Fluorination—A Useful Approach for the Isotopic Analysis of Hydrous Minerals," *Geochem. Cosmochim. Acta* **47**, 1589 (1983).

22. I.J. WINOGRAD, J.M. LANDWEHR, K.R. LUDWIG, T.B. COPLEN, and A.C. RIGGS, "Duration and Structure of the Past Four Interglaciations," *Quaternary Research* **48**, 141 (1997).

23. I.J. WINOGRAD, T.B. COPLEN, J.M. LANDWEHR, A.C. RIGGS, K.R. LUDWIG, K.R. SIMMONS, B.J. SZABO, P.T. KOLESAR, and K.M. REVESZ, "Continuous 500,000-Year Climate Record from Vein Calcite in Devils Hole, Nevada," *Science* **258**, 255 (1992).

24. J.A. APPS, "Hydrochemical Analysis," in *The Site-Scale Unsaturated Zone Model of Yucca Mountain, Nevada, for the Viability Assessment*, G.S. Bodvarsson, T.M. Bandurraga, and Y.S. Wu (eds.), Lawrence Berkeley National Laboratory Report LBNL-40376, Berkeley, California, Ch. 14 (1997).

25. L. BROWNING, W.M. MURHY, B.W. LESLIE, and W.L. DAM, *Thermodynamic Interpretations of Chemical Analyses of Unsaturated Zone Water from Yucca Mountain, Nevada, Scientific Basis for Nuclear Waste Management XXIII, Materials Research Society Symposium Proceedings **608***, R.W. Smith and D.W. Shoesmith (eds.), Materials Research Society, Warrendale, Pennsylvania, p. 237 (2000).

26. B.D. MARSHALL, L.A. NEYMARK, and Z.E. PETERMAN, "Estimation of Past Seepage Volumes from Calcite Distribution in the Topopah Spring Tuff, Yucca Mountain, Nevada," *Jour. Contaminant Hydrology* **62-63**, 237 (2003).

27. T.A. OLIVER and J.F. WHELAN, *Characterization of Seepage in the South Ramp ESF, Yucca Mountain, Nevada, Proc. Eleventh Int'l High-Level Radioactive Waste Management Conference, Las Vegas, Nevada, April 30-May 4, 2006*, American Nuclear Society, La Grange Park, Illinois (this volume).

28. J.P. ROUSSEAU, "Summary of Unsaturated-Zone Pneumatic System—Hydrogeology of the Unsaturated Zone, North Ramp Area of the Exploratory Studies Facility, Yucca Mountain, Nevada," J.P. Rousseau, E.M. Kwicklis, and D.C. Gillies (eds.), *U.S. Geological Survey Water-Resources Investigations Report* **98-4050**, 120 p. (1999).

29. D. GENTY and Y. QUINIF, "Annually Laminated Sequences in the Internal Structure of Some Belgian Stalagmites—Importance for Paleoclimatology," *Jour. Sedimentary Res.* **66**, 275 (1996).

30. L.A. AYLIFFE, P.C. MARIANELLI, K.C. MORIARTY, R.T. WELLS, M.T. MCCULLOCH, G.E. MORTIMER, and J.C. HELLSTROM, "500-Thousand-Year Precipitation Record from Southeastern Australia: Evidence for Interglacial Relative Aridity," *Geology* **26**, 147 (1998).

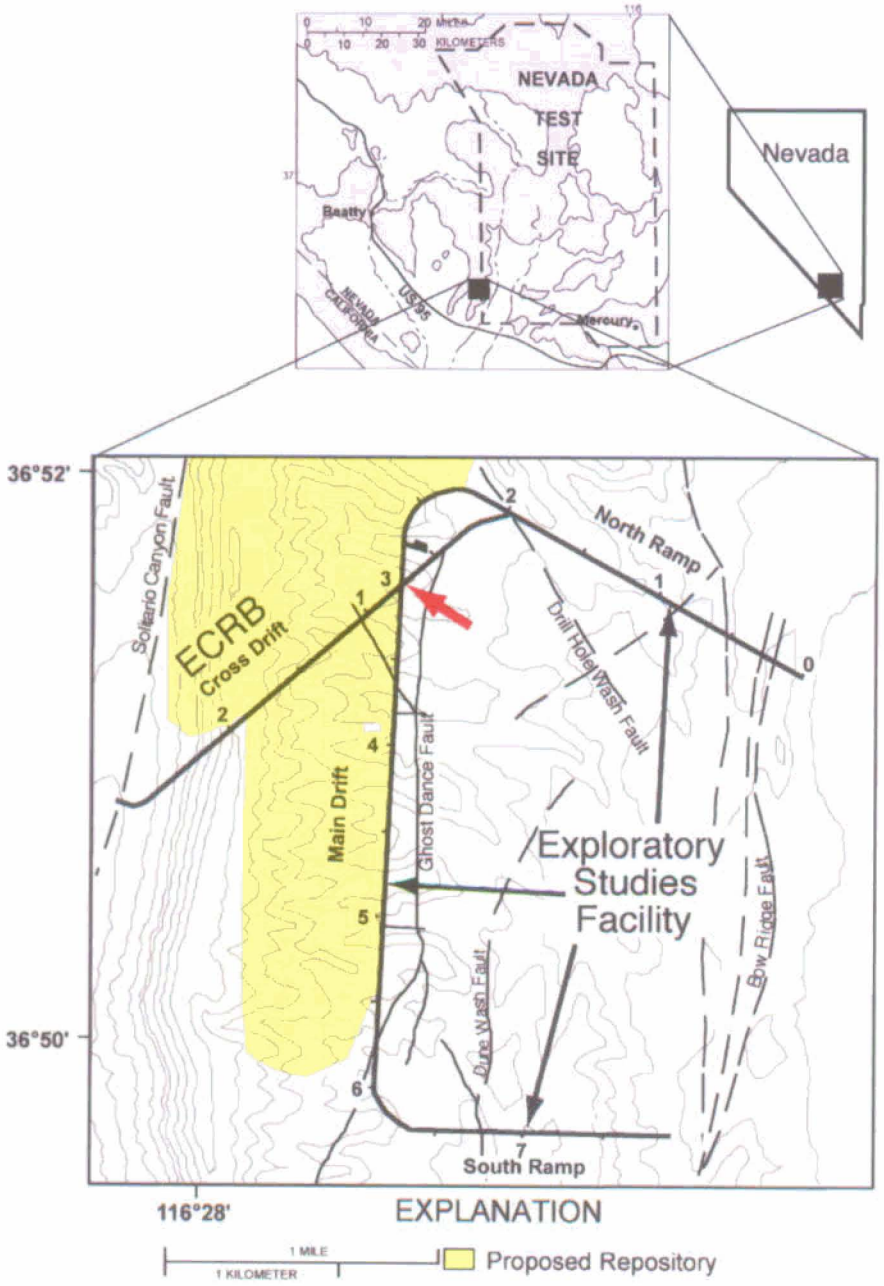

Fig. 1. Location of the Exploratory Studies Facility (ESF) and Enhanced Characterization of the Repository Block (ECRB) Cross Drift tunnels at Yucca Mountain, Nevada. Red arrow indicates approximate location of secondary mineral deposits discussed in the text and yellow shading indicates a portion of the footprint of the proposed underground repository. Bold numbers indicate kilometers from north portal in the ESF tunnel or entrance to the Cross Drift tunnel. In upper map, shaded areas indicate bedrock and white areas Quaternary sediments. Lower map after Day and others [1].

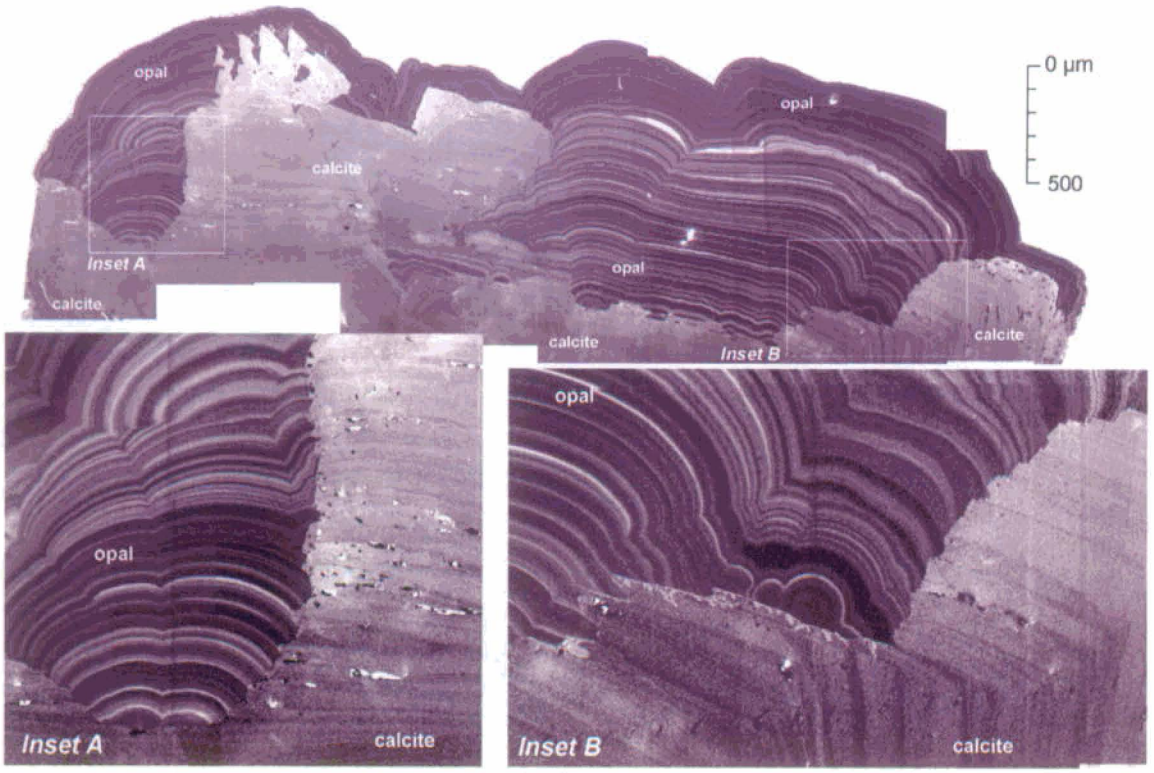

Fig. 2. Scanning electron microscope (SEM) cathodoluminescence (CL) images of late-stage opal and calcite from sample HD-2074 (ESF station 30+50.7, located 3050.7 meters from the north portal of the ESF) showing growth layering. Insets of areas with high-angle calcite-opal grain contacts show relations between opal and calcite CL microstratigraphy.

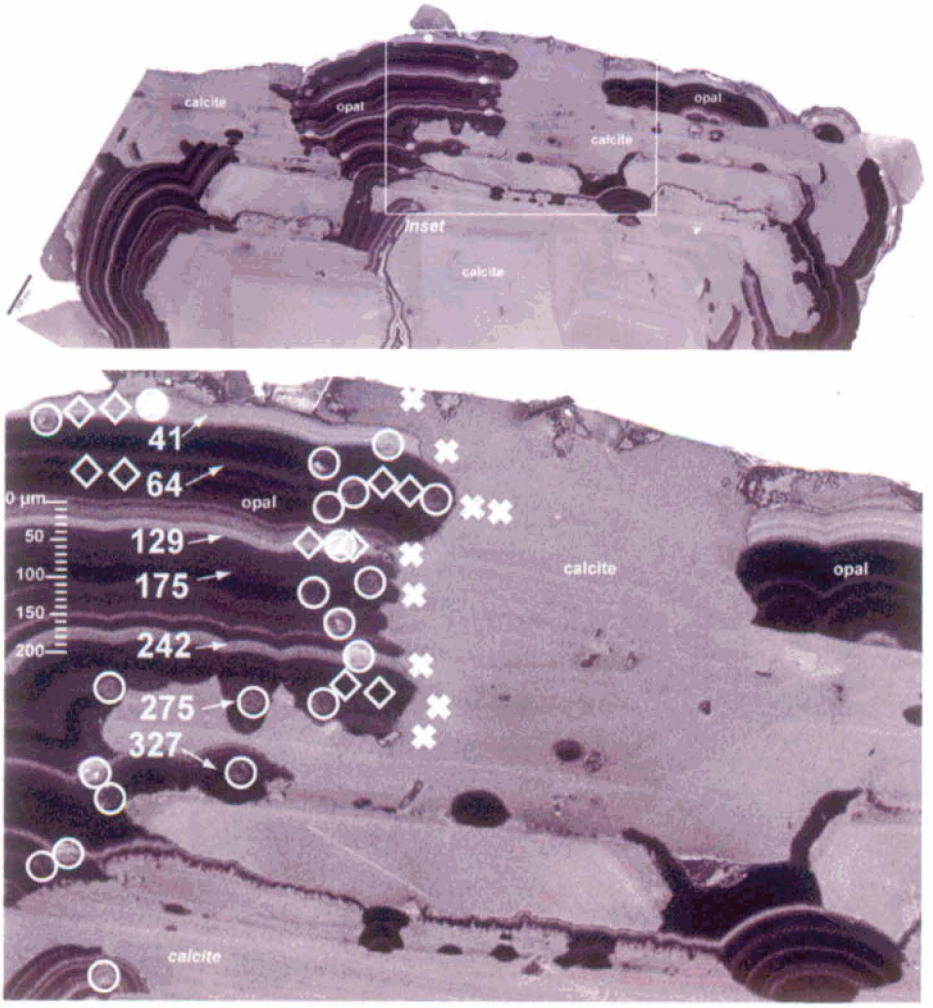

Fig. 3. Scanning electron microscope (SEM) cathodoluminescence (CL) images of late-stage opal and calcite from sample HD-2059 (ESF station 30+17.8, located 3017.8 meters from the north portal of the ESF), showing growth zoning and locations of secondary ion mass spectrometry (SIMS) analysis. Uranium (U)-series analyses are shown as circles, calcite delta oxygen-18 ($\delta^{18}O$) analyses as crosses, and opal $\delta^{18}O$ analyses as diamonds. U-series ages of several prominent opal layers are given in thousands of years (ka).

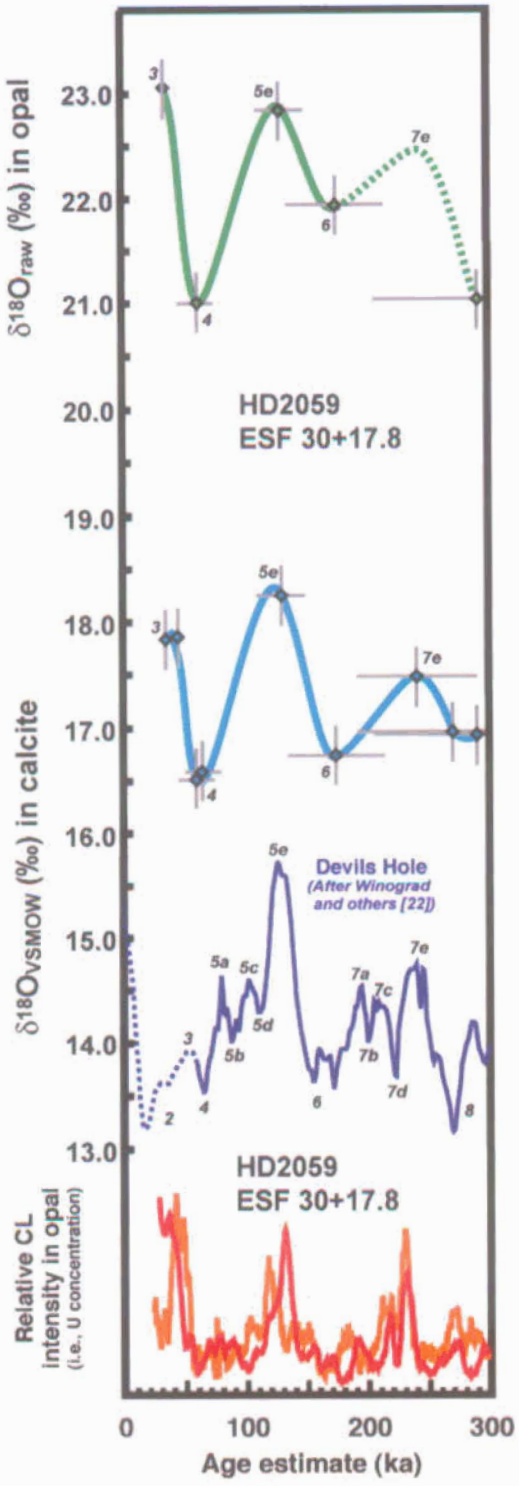

Fig 4. Age plotted against opal cathodoluminescence (CL) intensity (measured as pixel brightness from digital images and correlative with uranium (U) concentration) and delta oxygen-18 ($\delta^{18}O$) values for opal and calcite from unsaturated zone (UZ) mineral deposits at Yucca Mountain (sample HD-2059, ESF station 30+17.8, located 3017.8 meters from the north

portal of the ESF). Also shown for comparison are the temporal variations of calcite $\delta^{18}O$ values from the Devils Hole climate record (numbered glacial substage designations and dotted segment as shown in Fig. 7 of Winograd and others [22]). Dotted segment of opal $\delta^{18}O$ record reflects a data gap and is inferred from that of correlative calcite.

TABLE I. Paired delta oxygen-18 ($\delta^{18}O$) analyses of opal growth layers from sample HD-2059 (ESF station 30+17.8, located 3017.8 meters from the north portal of the ESF) by secondary ion mass spectrometry (SIMS).

ANALYSIS	$\delta^{18}O$ (‰)*
Opal layer 1	23.10, 23.09
Opal layer 2	22.02, 21.96
Opal layer 3	21.76, 21.64
Opal layer 4	22.73, 23.00
Opal layer 5	21.95, 21.82
Opal layer 6	22.10, 21.96
Opal layer 7	22.45, 22.37

* Uncorrected for instrumental mass fractionation.